

Fatigue Properties of Fine Grained Magnesium Alloys after Severe Plastic Deformation

Chin-Sung Chung

Bowon Light Metal Co., Hwasung-si, Kyungki-do 445-893, Korea

Duk-Kyu Chun, Ho-Kyung Kim*

*Department of Automotive Engineering, Seoul National University of Technology,
172 Kongnung-dong, Nowon-ku, Seoul 139-743, Korea*

Fine grained AZ31 and AZ61 magnesium alloys produced by equal channel angular pressing (ECAP) were tested for investigating tensile and fatigue properties, including microstructure, monotonic tensile flow, fatigue life and crack growth rate. For the two alloys, the yield stress of the ECAPed sample was lower than that of the unECAPed (=as received) sample, because of the fact that the softening effect due to texture anisotropy overwhelmed the strengthening effect due to grain refinement. Grain refinement of the AZ31 and AZ61 alloys through ECAP was found not to be significantly effective in increasing fatigue strength.

Key Words: Magnesium Alloys, Equal Channel Angular Pressing (ECAP), Fine Grained Microstructures, Fatigue Crack Growth Rate, Fatigue Strength

1. Introduction

Magnesium alloys have some advantage as a structural material in the automotive and aerospace industries due to their superior specific elastic modulus and specific strength, and so on (Friedrich and Schumann, 2001). Especially, wrought magnesium alloys have advantageous mechanical properties compared to cast magnesium ones. However, as a consequence of their hexagonal close packed (HCP) structure with a limited number of slip system, Mg alloys have principally been fabricated not by plastic forming but by casting such as die-casting and thixo-casting. Thus, it is required to improve the workability and strength of Mg alloys for their further applications to automotive engineering.

Recently, it was reported that grain refinement leads to improve the plastic formability and tensile properties. There have been only a limited number of studies on the fatigue behavior of fine grained materials. These studies have been mainly focusing on cyclic hardening or softening behavior with Bauschinger energy parameter and S-N curves for copper, aluminum alloys and steel (Agnew et al., 1999; Patlan et al., 2001; Rabinovich and Markushev, 1995; Kim et al., 2002). It is known that the fine grained materials have a higher resistance to crack initiation, which leads to increase in a high-cycle fatigue life. On the other hand, the fine grained materials are also known to exhibit a higher crack growth rate, which may result in a reduction in a low-cycle fatigue life (Patlan et al., 2001). Conflicting results are obtained in estimating fatigue properties. For example, fine grained Al 1560 alloy showed a shorter low-cycle fatigue life with some amount of improvement in the fatigue endurance (Rabinovich and Markushev, 1995). For the fine grained low carbon steel after equal channel angular pressing (ECAP), coarse and fine grained microstructures showed little difference in the

* Corresponding Author,

E-mail: kimhk@snut.ac.kr

TEL: +82-2-970-6348; FAX: +82-2-979-7032

Department of Automotive Engineering, Seoul National University of Technology, 172 Kongnung-dong, Nowon-ku, Seoul 139-743, Korea. (Manuscript Received January 5, 2005; Revised June 2, 2005)

fatigue crack growth behavior, despite the marked difference in ultimate tensile strength due to grain refinement (Kim et al., 2002). It implies that grain refinement does not appear to enhance the fatigue crack growth resistance of the fine grained steel. However, the Al 5056 alloy after ECAP treatment exhibited a longer high-cycle fatigue life while no improvement in the fatigue endurance observed (Patlan et al., 2001). Thus, this discrepancy might be partly due to processing methods and further thermomechanical treatment and structural parameters such as crystallographic texture and substructure.

The objective of this study is to develop a better understanding of tensile and fatigue properties of the AZ31 and AZ61 magnesium alloys, including microstructure, monotonic tensile flow, fatigue strength and crack growth rate. Emphasis is placed on investigating the fatigue properties of the fine grained magnesium alloys for their practical applications.

2. Experimental Procedures

ECAP processing was adopted in order to produce fine grained magnesium alloys. A commercial extruded Mg-Al Zn alloy, AZ31 and AZ61 alloys were cut to the rods with diameter of 14.5 mm and length of 90 mm. Their chemical compositions are given in Table 1. The alloys were solid-solution treated at 693 K for 2 hrs., and then quenched into room-temperature water. For the two alloys, ECAP was conducted using a die with an internal angle Φ of 90° and an outer curvature angle Ψ of 30° (see Fig. 1). The present die was designed to give an approximate strain ϵ of ~ 1 on each pressing. For all of the experiments, the ram speed was 5 mm/s. Repetitive pressings of the same sample were carried out. During ECAP, all pressings were conducted using the procedure designated as route Bc

(Yamashita et al., 1998), in which each sample was rotated 90° around its longitudinal axis between the passages. This route was applied since it has been demonstrated to be most effective in refining the microstructure to ultra-fine grain sizes with high-angle grain boundaries (Iwahashi et al., 1998). The Mg alloy rods were held at a pressing temperature for 10 min, and then pressed through the die preheated to the same temperature. For the AZ61 alloy, repetitive pressings of the same sample were performed up to 4 passes at the same temperature of 568 K. For the AZ31 alloy, the first and second pressings were conducted at 593 K whereas the third and fourth pressings were conducted at 523 K and 473 K, respectively, in order to confirm that a finer grain size is generally attained at a lower pressing temperature. The microstructure the AZ31 and AZ61 alloys were reasonably homogeneous and equiaxed after 4 pass, suggesting that dynamic recrystallization during pressing or static recrystallization during heating to processing temperature prior to subsequent pressing occurred. Figure 2 shows the optical photographs of (a) the 0 passed (= unECAPed), and (b) 4 pass ECAPed AZ31

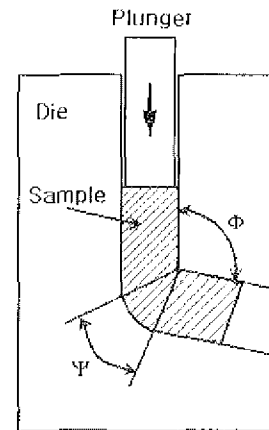


Fig. 1 Schematic illustration of the ECAP facility showing the angles Φ and Ψ

Table 1 Chemical composition of AZ31 and AZ61 alloys used for this study (wt.%)

Alloy	Al	Zn	Mn	Fe	Si	Cu	Ni	Mg
AZ31	2.56	0.89	0.39	0.007	0.02	0.006	0.003	bal
AZ61	6.13	0.71	0.18	0.003	0.02	0.008	0.004	bal

alloys. The average grain sizes of the unECAPed and 1, 2, 3, 4 pass ECAPed AZ31 and AZ61 alloy samples were presented in Table 1. The grains of the ECAPed AZ31 alloy were found to be bigger than those of the ECAPed AZ61 at the same pass number. The current ECAP technique proved an effective way in refining the AZ31 and AZ61 magnesium alloys.

Tensile and fatigue life (S-N) testing specimens with a 25 mm gauge length, 5 mm diameter, and 5 mm shoulder radius with the gauge length parallel to the longitudinal axis were cut out of the center portion of the unECAPed and ECAPed billets. Tensile test was conducted at room temperature under a constant cross-head speed of 5 mm/min, using a clip-on extensometer with a gage length of 12.7. Also, the fatigue life

experiments were carried out under the load ratio $R = \sigma_{min}/\sigma_{max} = 0.05$. Constant load amplitude fatigue crack growth experiments were carried out on the single edge-notched (SEN) sample with a thickness, width, and length of 3, 13 and 75 mm, respectively. The specimens were tested under load ratio $R = 0.05$ at a frequency of 20 Hz. All the tensile and fatigue tests were performed on a servo-hydraulic material test system (Instron 8511). A traveling microscope with a magnification of 50 was used for measuring crack length. The stress intensity factor for the SEN sample was calculated using the following equation :

$$K = \left(\frac{P}{Wt}\right) (\pi a)^{0.5} \left\{ 1.12 - 0.231 \left(\frac{a}{W}\right) + 10.55 \left(\frac{a}{W}\right)^2 - 21.72 \left(\frac{a}{W}\right)^3 + 30.39 \left(\frac{a}{W}\right)^4 \right\} \quad (1)$$

where W , t and a are the width and thickness of specimen and crack length, respectively. Vickers micro-hardness was measured on the plain perpendicular to the longitudinal axes (designated as X plane), by imposing a load of 500 g for 10 s.

3. Results and Discussion

3.1 Hardness and tensile properties

Figure 3 shows the variation of micro-hardness against $d^{-0.5}$ for the unECAPed (=0 pass) and

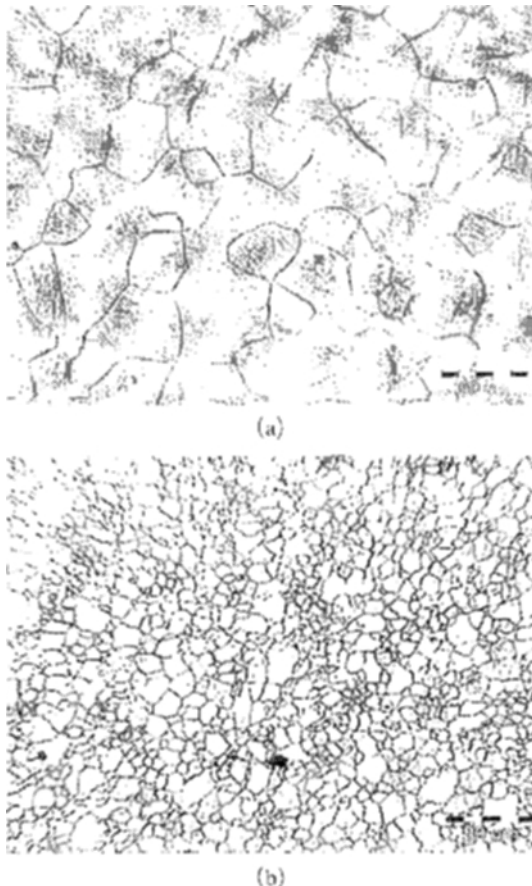


Fig. 2 Typical microstructure of (a) the unECAPed and (b) 4-pass ECAPed AZ31 alloys

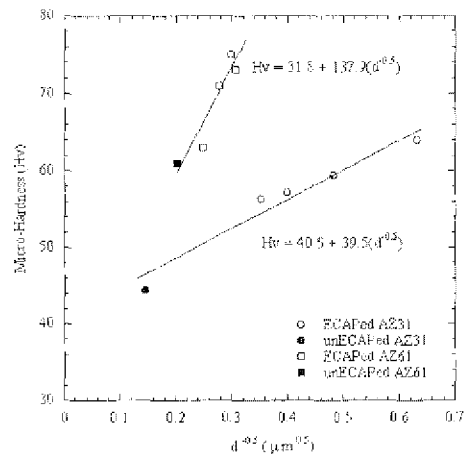


Fig. 3 Micro-hardness against $d^{-0.5}$ for the unECAPed and ECAPed magnesium alloys

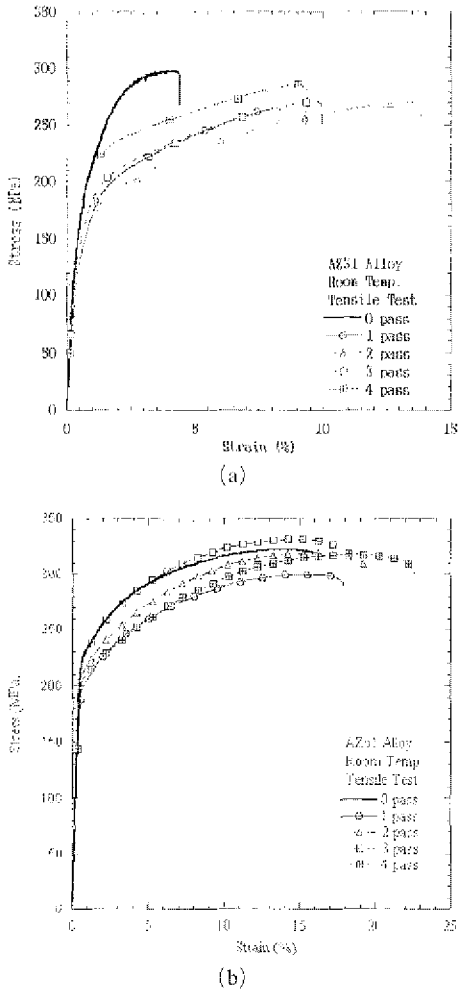


Fig. 4 Stress-strain curves for the unECAPed and ECAPed (a) AZ31 and (b) AZ61 alloys

ECAPed magnesium alloys where d is the average grain size. Hardness shows inverse proportion to the grain size, suggesting that the increase in the hardness can be directly due to the grain refinement.

Figure 4(a) and (b) show the engineering stress-strain curves of the unECAPed and ECAPed AZ31 and AZ61 alloys from 1 pass to 4 pass, respectively. Data for yield stress (YS), ultimate tensile strength (UTS), and elongation to failure were summarized in Table 2. From the tensile tests results, three important informations can be inferred. First, AZ61 alloy exhibits better mechanical properties than AZ31 alloy does, considering UTS, yield stress, hardness and elongation. Second, for the two alloys, yield stress of the ECAPed sample was lower than that of the unECAPed sample whereas the hardness of the former was higher than that of the latter. Third, for the two alloys, micro-hardness increased with grain refinement whereas the yield stress fluctuated with grain refinement. This inconsistency was not found in the report on the ECAPed Al alloys where a good correlation between YS and hardness was observed (Berbon et al., 1999).

The reason why the yield stress behavior does not agree with the hardness results is not clear at present. Though not well understood yet, it may be explainable by texture transition that occurs progressively during ECAP. Individual grains of the AZ31 and AZ61 alloys tend to develop a

Table 2 Room temperature mechanical properties of unECAPed and ECAPed AZ31 and AZ61 alloys

Condition	UTS (MPa)	Y.S (0.2%) (MPa)	Elongation (%)	Hardness (HV)	Grain Size (μm)
UnECAPed AZ31	298	201	4.3	45	48.3
1 passed AZ31	265	126	8.3	56	8.1
2 passed AZ31	270	126	13.8	57	6.3
3 passed AZ31	272	152	10.0	59	4.3
4 passed AZ31	287	180	9.4	64	2.5
UnECAPed AZ61	322	215	16.5	61	24.4
1 passed AZ61	302	193	17.9	63	16.2
2 passed AZ61	317	202	19.4	71	12.9
3 passed AZ61	329	208	17.7	75	11.2
4 passed AZ61	317	191	22.7	73	10.6

preferred orientation during ECAP, which results in texture development. At room temperature, primary slip occurs on the (0001) basal plane and in the most closely packed direction of the plane in Mg. For pure Mg and Mg alloys, basal planes tend to lie parallel to the extrusion direction after extrusion (Kim et al., 2002), indicating that slip on the basal plane would be difficult and the strength increases with limited non-basal slip activities. Kim et al. (2002) reported on the ECAPed AZ61 alloys that the Schmid factor on (0001) basal planes was increased by the rotation of the basal poles to approximately 45° from the extrusion axis during ECAP and thus a lower stress was needed for yielding. The largely increased tensile ductility after ECAP, on the other hand, could be related to the large strain-hardening after yielding and the hardening was attributed to the activation of two or more slip planes as the consequence of rotation of slip planes during ECAP (Kim et al., 2002). It seems that the strengthening effect by grain refinement is more pronounced than the softening effect by texture anisotropy in hardness testing where deformation occurs locally and non-uniformly, whereas the softening effect by texture anisotropy is more dominant in tensile testing where deformation occurs more macroscopically and uniformly.

3.2 Fatigue properties

Figure 5 is the S-N curves for the unECAPed and 4 pass ECAPed AZ31 and AZ61 alloys. In case of the AZ31 alloy, the ECAPed sample exhibits a reduction of fatigue life (more than a factor of 10) in both low and high-cyclic fatigue region ($10^4 < N < 10^7$), compared to the unECAPed sample. The ECAPed sample has about 13% reduction in fatigue endurance life at $N=10^7$. The ultimate tensile and yield strengths of the ECAPed sample are lower than those of the unECAPed. Comparison of the fatigue behavior between the unECAPed and ECAPed samples indicates that the fatigue life has a correlation with the yield strength in AZ31 alloy. In case of the AZ61 alloy, the unECAPed sample exhibits a slightly better fatigue life than the ECAPed sample does in low cycle fatigue region ($10^4 < N < 3 \times 10^5$) whereas

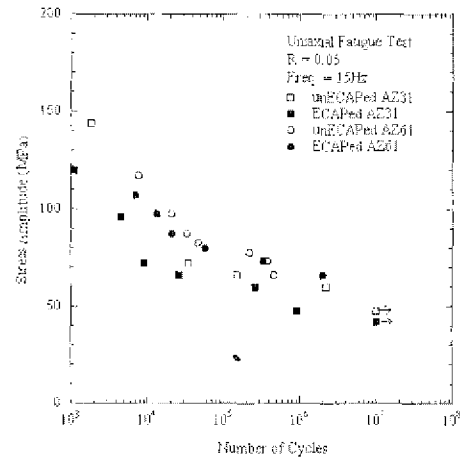


Fig. 5 The S-N curves for the unECAP and ECAPed AZ31 and AZ61 alloys

the unECAPed sample exhibits a small reduction of fatigue life in high cycle region, compared to the ECAPed sample.

The fatigue life under cyclic loading consists of two phases, the crack initiation period followed by a crack growth period up to failure. The crack initiation period may govern the fatigue life under high-cycle fatigue. The higher yield stresses in the unECAPed AZ31 and AZ61 alloy samples prevented macroscopic plastic deformation at the beginning of load controlled cycling in contrast to the ECAPed samples, resulting in increasing the crack initiation period. Thus, the reduction of fatigue strength for the ECAPed sample may be mainly caused by the reduction of crack nucleation resistance, resulting from lower yield strength. Even though it is necessary to attain more fatigue data to understand fatigue strength after ECAP process, it can be concluded that grain refinement of the AZ31 and AZ61 alloys through ECAP seems not to be significantly effective in increasing fatigue strength.

Fatigue crack growth rate (da/dN) curves of the unECAPed and 4 pass ECAPed AZ31 samples at load ratio of $R=0.05$ are presented in Fig. 6. It clearly shows that the crack growth rate in the ECAPed sample with fine microstructures appears to be lower than that in the unECAPed sample with a coarse microstructure at the same load ratio. This is different from the behavior of

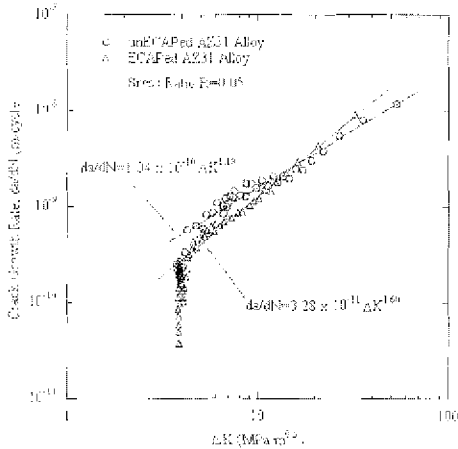


Fig. 6 A comparison of fatigue crack growth behavior of the unECAPed and ECAPed AZ31 alloys

other ECAPed Al and steel alloys, in which finer microstructures exhibit higher growth rates (Kim et al., 2002; Vinogradov et al., 1999). However, at $\Delta K > 20 \text{ MPa}\sqrt{m}$, the crack growth rate in the ECAPed sample was higher than that of in the unECAPed one. It also shows that the ΔK_{th} value for the ECAPed sample ($3.82 \text{ MPa}\sqrt{m}$) is actually very close to that for the unECAPed ($3.74 \text{ MPa}\sqrt{m}$) one even though the growth rate curves do not reach threshold levels experimentally. In the stage II regime of the growth rate curves, the crack growth behavior at two load ratios apparently conforms to the Paris relationship as follows:

$$da/dN = C(\Delta K)^m \tag{2}$$

The values of the constants, C and m were calculated from the stage II regime of the curves and summarized in Table 3. The slope of the ECAPed sample is different from that of the unECAPed one.

Fine grained materials are known to exhibit a lower resistance of fatigue crack growth. Because the plastic deformation zone in the fine grained

materials is normally larger than the grain size, a reverse slip of the dislocations during unloading is often impossible so that the accumulation of damage is large during cycling (Rabinovich and Markushev, 1995). The crack growth resistance of the present investigation exhibited conflicting results, unlike other ultrafine grained materials which have a lower threshold and higher fatigue crack growth rates, compared to coarse grained materials (Rabinovich and Markushev, 1995; Vinogradov et al., 1999). It is not clear why the ECAPed AZ31 alloy with a finer grain size exhibited higher crack threshold and lower crack growth rate. It seems that enhanced ductility due to grain refinement in the ECAPed AZ31 alloy resulted in increasing crack growth resistance because of its better ability to accommodate plastic strains during cycling. Thus, the influence of grain size on the fatigue properties seems to be very complex due to the interaction between several intrinsic and extrinsic factors.

Fractography for the unECAPed and ECAPed AZ31 alloy samples at different load ratios was observed using SEM. The present ECAPed samples showed only minimal differences in the fractography for the two different load ratios. Scanning electron micrographs of the fatigue fracture surfaces of the unECAPed and ECAPed AZ31 alloy samples are shown in Figs. 7(a) and (b), respectively, at intermediate growth rates (at $R=0.05$ and $\Delta K \sim 7 \text{ MPa}\sqrt{m}$). In Fig. 7(a), the unECAPed sample showed irregular surfaces going up and down in some random way. In contrast, the ECAPed fracture mode is mostly faceted and brittle-like.

Commonly, five mechanisms can be taken into account concerning fatigue crack closure phenomena (Suresh and Ritchie, 1984): plasticity-induced closure, oxide-induced closure, roughness-induced closure, transformation-induced closure, and viscous fluid pressure induced closure. For the current unECAPed and ECAPed AZ31 alloy, no phase transformation occurred during fatigue, and viscous fluid was absent. Also, the oxide-induced crack closure was excluded because fretting debris was not found on the surfaces. Thus, plasticity-induced and roughness-induced crack

Table 3 Results of regression of da/dN versus ΔK plots for the AZ31 alloy

Material	R	C (m/cycle)	m
unECAPed	0.05	1.04×10^{-10}	1.20
ECAPed	0.05	3.28×10^{-11}	1.60

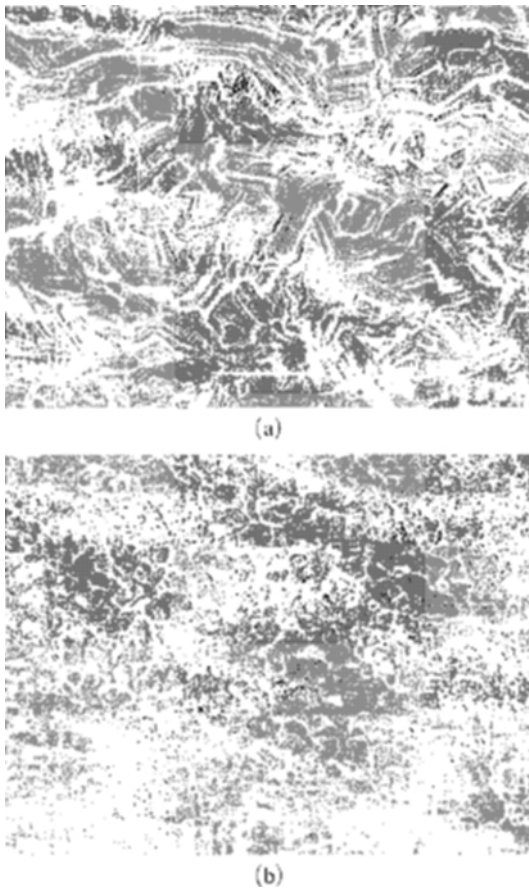


Fig. 7 Fatigue crack surfaces at $K \sim 7 \text{MPa}\sqrt{m}$ for (a) the unECAPed and (b) ECAPed samples of the AZ31 alloy. Crack propagation direction is from left to right

closure were considered to be factors influencing fatigue crack growth behavior of both the AZ31 alloy samples. It is impossible to evaluate quantitatively the effects of the plasticity-induced and roughness-induced crack closure from current experiment data.

Assuming crack growth per cycle is proportional to crack tip opening displacement (CTOD) due to plasticity-induced crack closure, crack growth rate can be described by Dugdale's model (Dugdale, 1960)

$$da/dN \approx \Delta \text{CTOD} \approx \Delta K^2 / \sigma_y E \quad (3)$$

where ΔK is the range of stress intensity ratio and E is the Young's modulus. Lower yield stress causes smaller ΔCTOD of fatigue cracks under

the same stress intensity factor condition. This may in turn lead to an increase in the crack growth rates. However, the crack growth rate in the ECAPed sample with lower yield strength ($=180 \text{MPa}$) exhibited lower than that in the unECAPed one with higher yield strength ($=201 \text{MPa}$) at low ΔK regime. Thus, the plasticity-induced crack closure effect was considered to be a minor factor controlling the growth rate in the crack growth rate of the AZ31 samples. We should also notice that at low crack growth rate regime, where the effect of the roughness-induced crack closure is significant, the crack growth rate in the coarse grained unECAPed sample with rough fracture surfaces was higher than that in the fine grained ECAPed one with flat fracture surfaces. Thus, it can be concluded that both the plasticity-induced and roughness-induced crack closure effects were minor factors governing the growth rate in the crack growth rate of the AZ31 alloy sample, especially at low ΔK regime.

4. Conclusions

Fine grained AZ31 and AZ61 Mg alloys produced by ECAP were tested for investigating tensile and fatigue properties, including microstructure, monotonic tensile flow, fatigue life and crack growth rate. Hardness shows inverse proportion to the grain size, suggesting that the increase in the hardness can be directly due to the grain refinement. For the two alloys, the yield stress of the ECAPed sample was lower than that of the unECAPed sample, because of the fact that the softening effect due to texture anisotropy overwhelmed the strengthening effect due to grain refinement. The ECAPed sample with a finer grain size exhibited a lower crack growth rate than the unECAPed one. However, grain refinement of the AZ31 and AZ61 alloys through ECAP seems not to be significantly effective in increasing fatigue strength.

References

Agnew, S. R., Vinogradov, A. Y., Hashimoto, S. and Weertman, J. R., 1999, "Overview of Fa-

tigue Performance of Cu Processed by Severe Plastic Deformation," *J. Electronic Mater.*, Vol. 28, No. 9, pp. 1038~1044.

Berbon P. B., Nikolai, K. T., Valiev, R. Z., Furukawa, M., Horita, Z., Nemoto, M. and Langdon, T. G., 1998, "Fabrication of Bulk Ultrafine-Grained Materials Through Intense Plastic Straining," *Metal. Mat. Trans.*, Vol. 30A, pp. 1998-2237.

Dugdale, D. S., 1960, "Yielding of Steel Sheets Containing Slits," *J. Mechanics and Physics of Solid*, Vol. 8, pp. 100~104.

Friedrich, H. and Schumann, S., 2001, "Research for a New Age of Magnesium in the Automotive Industry," *J. Mat. Processing Tech.*, Vol. 117, pp. 276~281.

Iwahashi, Y., Horita, Z., Nemoto, M. and Langdon, T. G., 1998, "The Process of Grain Refinement in Equal-Channel Angular Pressing," *Acta Mater.*, Vol. 46, pp. 3317~3331.

Kim, H. K., Choi, M. I., Chung, C. S. and Shin, D. H., 2002, "Fatigue Crack Growth Behavior in Ultrafine Grained Low Carbon Steel," *KSME Int. J.*, Vol. 16, No. 10, pp. 1246~1252.

Kim, W. J., An, C. W., Kim, Y. S. and Hong, S. I., 2002, "Mechanical Properties and Microstructures of an AZ61 Mg Alloy Produced by Equal

Channel Angular Pressing," *Scripta Mater.*, Vol. 47, pp. 39~44.

Patlan, V., Vinogradov, A., Higashi, K. and Kitagawa, K., 2001, "Overview of Fatigue Properties of Fine Grain 5056 Al-Mg Alloy Processed by Equal-Channel Angular Pressing," *Mater. Sci. & Eng.*, Vol. A300, pp. 171~182.

Rabinovich, M. K. H. and Markushev M. V., 1995, "Influence of Fine Grained Structure and Superplastic Deformation on the Strength of Aluminum Alloys," *J. Mater. Sci.*, Vol. 30, pp. 4692~4702.

Suresh, S. and Ritchie, R. O., 1984, "Propagation of Short Fatigue Cracks," *Int. Metal. Rev.*, Vol. 29, pp. 445~476.

Vinogradov, A., Nagasaki, S., Patlan, V., Kitagawa, K. and Kawazoe, M., 1999, "Fatigue Properties of 5056 Al-Mg Alloy Produced by Equal-Channel Angular Pressing," *NanoStructured Mat.*, Vol. 11, No. 7, pp. 925~934.

Iwahashi, Y., Furukawa, M., Horita, Z., Nemoto, M. and Langdon, T. G., 1998, "Microstructural Characteristics of Ultrafine-Grained Aluminum Processed Using Equal-Channel Angular Pressing," *Metal. Mat. Trans.*, Vol. 29A, pp. 2245~2252.